



Cite this: *Nanoscale Adv.*, 2025, **7**, 7109

Interfacial engineering of nano-copper: mechanisms, strategies, and innovations for oxidation resistance

Bo Zhang,^a Ziyin Zhou,  ^{*a} Jing Huang,^b Jiani Zhan,^a Qiuyu Yao,^a Rui Lu,^a Ruixu Hu^a and Bohong Zhu^a

Nano-copper, characterized by its unique physicochemical properties such as high specific surface area, quantum size effects, and exceptional conductivity, has emerged as a pivotal material in advanced technologies. However, its susceptibility to oxidation under ambient conditions significantly compromises its performance and limits practical applications. This review systematically examines the oxidation mechanisms of nano-copper, emphasizing the roles of particle size, temperature, crystallographic orientation, and environmental factors (e.g., humidity and oxygen adsorption). Key findings reveal that oxidation follows distinct pathways in dry *versus* humid environments, with electrochemical corrosion accelerating degradation in the presence of moisture. To address these challenges, recent advancements in surface modification strategies are comprehensively reviewed. Coating technologies, including graphene encapsulation and carbon-based composites, demonstrate enhanced oxidation resistance by physically isolating nano-copper from reactive species. Core–shell architectures, such as Cu@Ni and Cu@Ag, leverage electronic shielding and interfacial engineering to improve stability. Functional group modifications (e.g., –SH and –COOH) and coordination layer designs (e.g., ligand complexes) achieve molecular-level control over surface passivation, while complexation methods utilize ligands for eco-friendly stabilization. Despite progress, challenges persist in achieving uniform shell layers, scalable fabrication, and long-term durability. Future research directions emphasize the development of low-cost, green synthesis techniques, atomic-scale interface engineering, and multifunctional nano-copper. Innovations such as dynamic coordination systems, self-healing coatings, and crystallographic orientation-specific modifications hold promise for expanding nano-copper's applicability in flexible electronics, catalysis, and biomedical fields. This review underscores the critical need for interdisciplinary approaches to translate laboratory-scale breakthroughs into industrial solutions, ultimately unlocking the full potential of nano-copper in next-generation technologies.

Received 27th July 2025
Accepted 24th September 2025

DOI: 10.1039/d5na00716
rsc.li/nanoscale-advances

1. Introduction

In the continuous advancement of materials science, nano-materials have emerged as a research focus due to their unique performance advantages. Nano-copper, as a typical representative, exhibits distinct characteristics and application potential compared to traditional copper materials. Nano-copper refers to copper particles or structural materials with particle sizes in the range of 1–100 nanometers (nm),¹ approaching atomic or molecular dimensions. This scale endows it with exceptional physical, chemical, and mechanical properties, leading to significant differences from conventional bulk copper (ordinary copper) and micron-scale copper (micro-copper).

^aCollege of Materials and Advanced Manufacturing, Hunan University of Technology, Zhuzhou, Hunan, 412000, China. E-mail: Zhou102443@outlook.com

^bDepartment of Chemistry and Chemical Engineering, Hunan Normal University, Changsha, Hunan, 410081, China

From a comparative perspective, nano-copper demonstrates an extremely high specific surface area ($50\text{--}200\text{ m}^2\text{ g}^{-1}$) and strong surface activity, manifesting as rapid oxidation and high catalytic activity. Its conductivity is excellent, with a resistivity as low as $3\text{ }\mu\Omega\text{ cm}$, and it exhibits high strength and hardness due to nanocrystalline strengthening effects.² However, it suffers from poor oxidation resistance. In contrast, micro-copper (1–100 μm) has a lower specific surface area ($0.1\text{--}1\text{ m}^2\text{ g}^{-1}$), moderate surface activity requiring high-temperature activation, medium conductivity comparable to that of bulk copper, average mechanical performance, and relatively stable surface oxide layers.³ Ordinary copper (bulk material) has an extremely low specific surface area ($<0.01\text{ m}^2\text{ g}^{-1}$), weak surface activity necessitating treatment with strong acids or oxidizers, standard conductivity ($1.68\text{ }\mu\Omega\text{ cm}$), low strength, high ductility, and a tendency to oxidize into CuO or Cu₂O.^{4,5} These differences in properties dictate their divergent applications across various fields.

In the electronics field, nano-copper leverages its unique surface effects and quantum size effects to produce high-performance conductive pastes, enabling the formation of precise and highly conductive circuits on printed boards.^{6,7} In chemical production, nano-copper serves as a catalyst with high catalytic activity, enhancing production efficiency and reducing energy consumption.^{8,9} In the medical industry, nano-copper exhibits inhibitory and bactericidal effects against various pathogens, making it widely applicable in antibacterial applications^{10,11} and even potential treatments for neuroblastoma.¹² Additionally, it shows promise in spectroscopy,^{13,14} preservatives,¹⁵ sensors,^{16,17} and lubricants.^{18,19}

In contrast, micro-copper and ordinary copper have long dominated traditional industrial sectors. For example, ordinary copper, owing to its excellent conductivity and processability, remains the preferred material for power transmission in wire and cable manufacturing.²⁰ Micro-copper, on the other hand, is utilized in powder metallurgy to fabricate complex-shaped components for machinery manufacturing and acts as a conductive filler to improve the electrical performance of composites, finding extensive use in electronic packaging and related fields.²¹

Although micro-sized copper and ordinary copper dominate traditional industries, they fall short of meeting the demands of cutting-edge technologies. For instance, in the aerospace sector, aircraft must operate under extreme conditions, necessitating materials with exceptional strength, lightweight properties, and high-temperature resistance.²² Similarly, in the field of electronic chip manufacturing, the pursuit of faster computing speeds and smaller chip sizes requires materials with ultra-high electrical conductivity and precise microstructures.²³ Due to their inherent limitations, micron-sized copper and ordinary copper are unable to fulfill these high-tech requirements. Specifically, ordinary copper underperforms in terms of strength and lightweight properties, making it unsuitable for aerospace structural components. Meanwhile, micron-sized copper exhibits insufficient electrical conductivity and surface activity in certain advanced electronic applications, thereby hindering further breakthroughs in related technologies (Table 1).

However, nano-copper is highly prone to oxidation in air, particularly under harsh conditions such as high temperatures

and humidity, leading to surface degradation. In terms of electrical conductivity, the originally outstanding conductive properties of nano-copper deteriorate due to oxidation.²⁴ The copper oxide compounds formed on its surface after oxidation act as semiconductors or insulators, hindering efficient electron transport.²⁵ This compromises its conductivity in electronic devices, ultimately reducing overall circuit performance. Regarding mechanical properties, oxidation alters the internal structure of nano-copper, weakening atomic bonding forces and diminishing its strength and hardness. This significantly undermines the advantages of high strength and hardness derived from its nanocrystalline strengthening effect. Furthermore, oxidation weakens the adhesion between nano-copper and other materials. In scenarios involving composite material fabrication or multi-material integration, this impaired bonding capability compromises the overall performance and stability of composite systems. Additionally, oxidation of nano-copper raises environmental and health concerns.²⁶ Should oxidized nano-copper enter natural ecosystems, its altered chemical properties could potentially exert unforeseen impacts on soil, water bodies, and broader ecological systems.^{27,28}

This exceptionally high reactivity severely restricts the service life and application scope of nano-copper. Consequently, surface modification of nano-copper to improve its oxidation resistance has emerged as a focal research area in materials science. This article concentrates on modification methods for nano-copper, offering a systematic and comprehensive overview of advancements in coating technologies, core–shell structure fabrication, functional group functionalization, complexation-based modifications, and coordination-layer engineering. Each method is analyzed in detail to highlight its contributions to enhancing the material's stability and applicability.

2. Oxidation behavior of nano-copper

Nano-copper, characterized by its small particle size and large specific surface area, exhibits high sensitivity to atmospheric oxygen and strong surface reactivity, making it prone to adsorbing oxygen and water from the air—two key factors driving atmospheric corrosion. The oxidation of nano-copper is

Table 1 Comparison of nano-copper, micro-copper, and ordinary copper

Property	Nano-copper (1–100 nm)	Micro-copper (1–100 µm)	Bulk copper
Specific surface area	Very high (50–200 m ² g ⁻¹)	Low (0.1–1 m ² g ⁻¹)	Extremely low (<0.01 m ² g ⁻¹)
Surface activity	Very strong (prone to oxidation and high catalytic activity)	Moderate (requires high-temperature activation)	Weak (requires strong acid/oxidizer treatment)
Conductivity	High (low resistivity: 3 µΩ cm)	Moderate (close to that of bulk copper)	Standard (1.68 µΩ cm)
Mechanical properties	High strength/hardness (nanocrystalline strengthening effect)	Moderate (larger grain size)	Low strength and high ductility
Oxidation resistance	Poor (requires surface coating/modification)	Moderate (stable surface oxide layer)	Easily oxidized (forms CuO/Cu ₂ O)
Applications	Conductive inks, catalysts, antibacterial materials, <i>etc.</i>	Powder metallurgy, conductive fillers, thermal interface materials, <i>etc.</i>	Wires, pipes, <i>etc.</i>



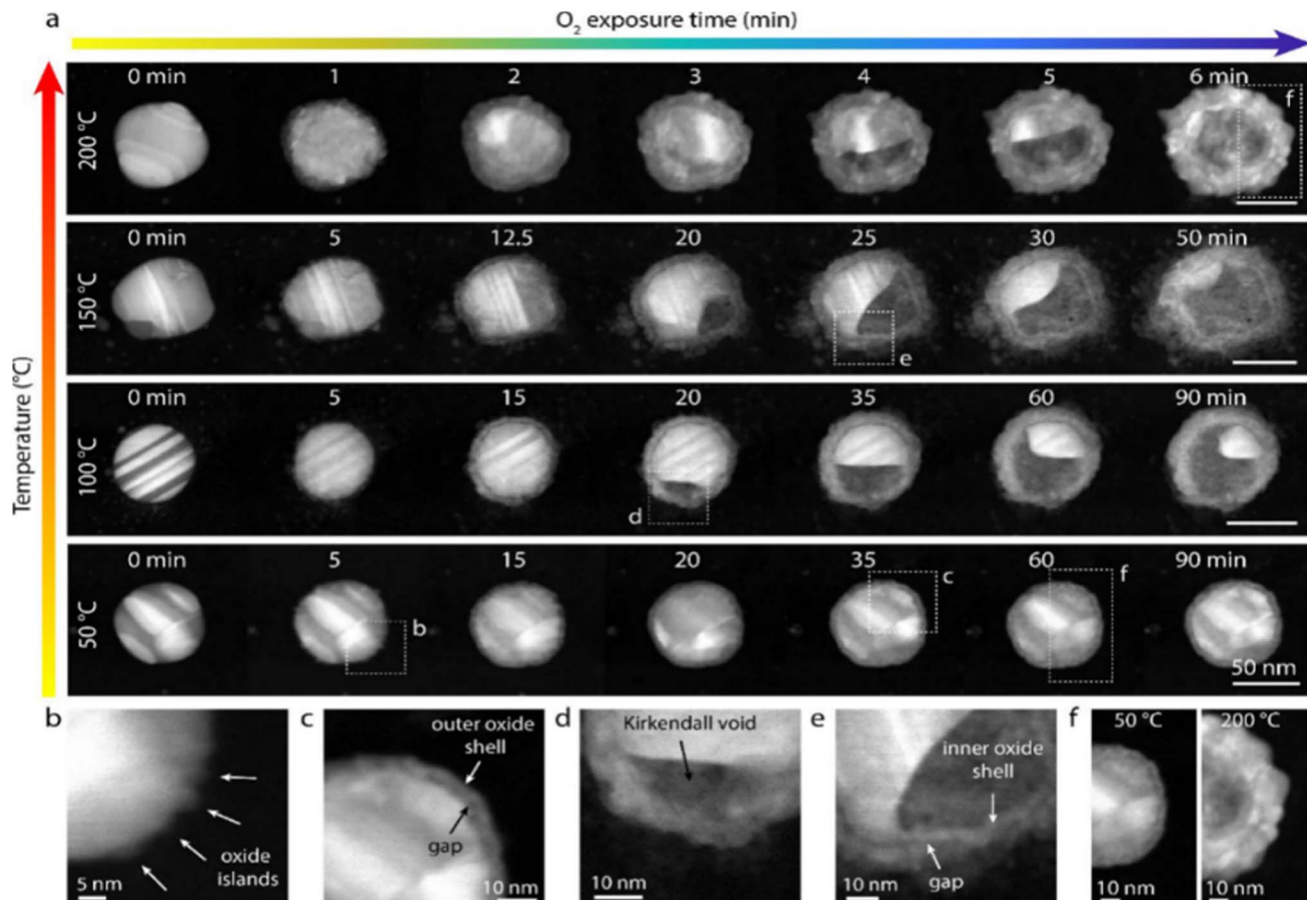


Fig. 1 ADF STEM of single Cu particle oxidation at different temperatures. (a) ADF STEM images acquired during the oxidation of Cu nanoparticles at 50, 100, 150 and 200 °C, in 3 mbar O₂, after different O₂ exposure times (indicated in the images). The scale bars are 50 nm. Specifically relevant features are highlighted: (b) the nucleation of oxide islands on the metallic surface at the initial stage of oxidation, (c) the formation of a homogeneous outer oxide shell after oxide island coalescence, and the vacancy gap layer between the outer shell and the metal core, (d) the typical NK void nucleation site at the metal – gap layer interface, (e) the inner oxide shell formed inside the particle and separated from the outer oxide shell by the vacancy gap layer, and (f) a comparison of the oxide morphology for oxidation at 50 °C (left) and 200 °C³¹.

influenced by various parameters, including particle size and temperature.²⁹

Particle size significantly impacts nano-copper oxidation. Leitner *et al.*³⁰ through comparative studies on the oxidation of nano-copper and microparticles of varying sizes demonstrated that nano-copper oxidizes more readily than its micrometer-sized counterparts, a phenomenon governed by kinetic rather than thermodynamic factors in the oxidation reaction.

Temperature exerts a significant influence on nano-copper oxidation. In their research, Nilsson *et al.*³¹ monitored the oxidation process of individual Cu nanoparticles at varying temperatures using *in situ* environmental scanning transmission electron microscopy (STEM). At 50 °C, Cu₂O oxide islands were observed to nucleate and grow on the particle surface, eventually merging into a uniform oxide layer. This process aligns with the Cabrera–Mott mechanism, resulting in a self-limiting oxide layer thickness of 5.5 ± 0.7 nm. At higher temperatures (100–200 °C), in addition to outward oxide layer growth, inward oxide layer formation occurred following the

Valensi–Carter mechanism, with oxidation rates accelerating as temperature increased. These distinct oxidation behaviors across temperature regimes are clearly illustrated in Fig. 1.

The oxidation process of nano-copper involves unique phenomena such as the Kirkendall effect and void formation. In their study, Nilsson *et al.*³² investigated the oxidation of individual Cu nanoparticles using *in situ* plasmonic nanospectroscopy combined with electrodynamic simulations. They observed uniform growth of the oxide shell during the initial oxidation stage. However, when the oxidation fraction reached approximately 0.3–0.4 (Fig. 2), Kirkendall voids began to form, accompanied by characteristic peak splitting in the single-particle scattering spectra. Additionally, Zuo *et al.*³³ while studying oxidation effects in sintered Cu nanoparticle interconnects during high-temperature aging uncovered a novel mechanism of oxidation-mediated nanovoid formation along grain boundaries. They attributed this phenomenon to the differential diffusion rates of Cu and oxygen atoms through the thin oxide layer, a behavior analogous to the Kirkendall effect.



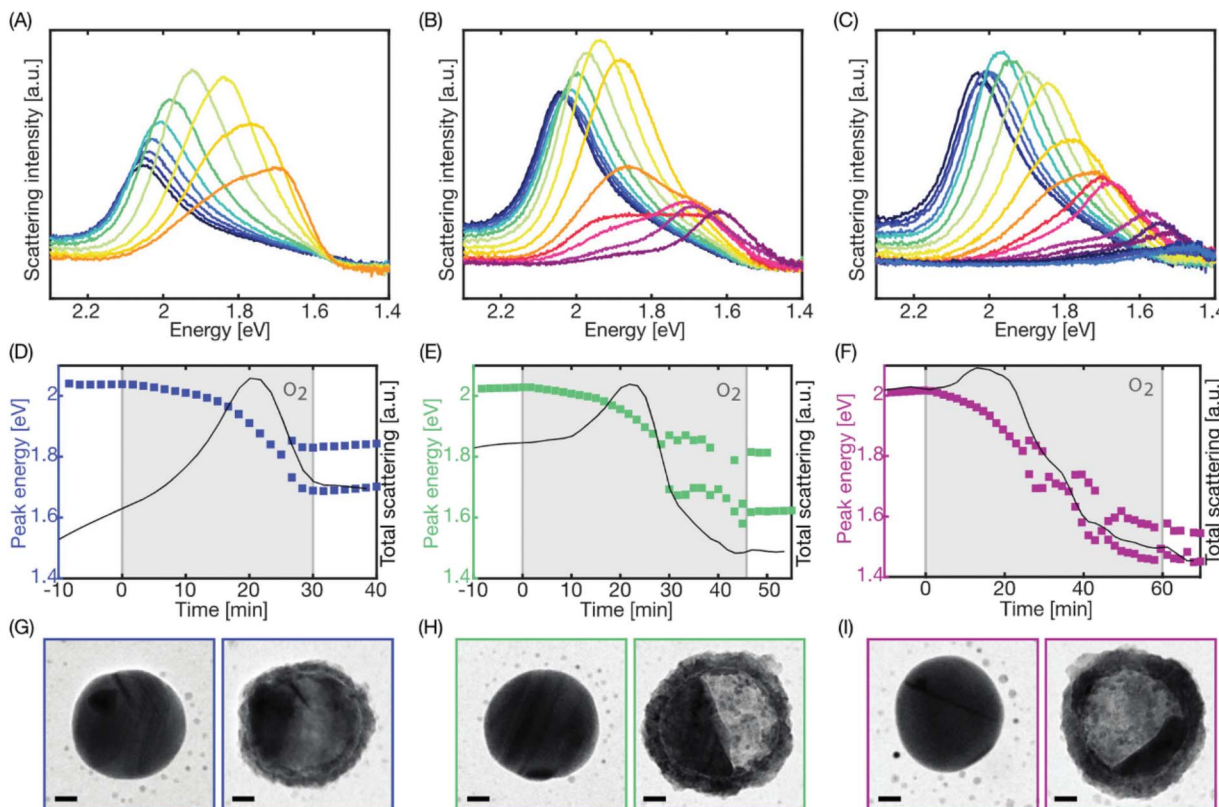
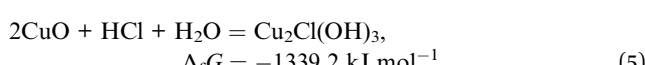
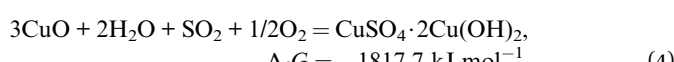
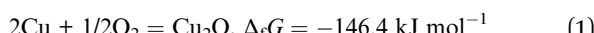


Fig. 2 Single particle optical response during oxidation. The optical scattering spectra collected from three individual Cu nanoparticles during (A) 30 minutes, (B) 45 minutes and (C) 60 minutes of oxidation, respectively, all in 1% O₂ at 150 °C. Spectra recorded every 200 seconds are plotted for each nanoparticle to show their evolution over time as oxidation progresses. Note the reversed energy scale on the x-axis. (D–F) The peak energy (left axis) and the integrated peak intensity (right axis) of the scattering spectra of the same three nanoparticles plotted every 100 seconds. The grey shaded area indicates the 1% O₂ interval lasting 30 min, 45 min or 60 min, respectively. After approximately 25 minutes of oxidation, the peak splits into two modes for all three nanoparticles, which can also be seen in (A–C). (G–I) TEM images of the same three nanoparticles obtained before (left) and after oxidation (right). The scale bars are 20 nm.³²

This mechanism highlights how localized oxidation at grain boundaries drives structural degradation in nanoscale copper systems.

Atmospheric corrosion is one of the primary corrosion forms of copper. According to the principles of atmospheric corrosion, the oxidation mechanisms of copper powder differ significantly in dry and humid environments.²⁹ The Gibbs free energies necessary for the formation of typical copper corrosion products are outlined as follows:

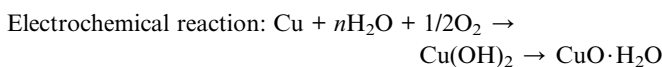
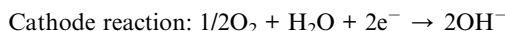


In dry environments, where no water film exists on the copper surface, oxidation relies solely on adsorbed oxygen,

following chemical reaction principles, and progresses at a relatively slow rate. Initially, a thin oxide layer (Cu₂O) forms on the copper surface. As the reaction proceeds, the oxide layer thickens, with Cu₂O dominating the inner layer and CuO forming the outer layer. Siti Rahmah Esa *et al.*³⁴ discovered that the sequence of copper surface oxidation involves oxygen chemisorption, nucleation and growth of surface oxides, and bulk oxide growth. At high temperatures (600–800 °C), oxidation is controlled by the diffusion of copper atoms through the Cu₂O lattice, whereas at lower temperatures (around 300 °C), it primarily occurs *via* Cu₂O grain boundary diffusion. During oxidation, copper first forms Cu₂O, which further oxidizes to CuO. This process involves ion and electron migration: cation migration leads to oxide layer formation at the air interface, while anion migration occurs at the metal-oxide interface.

In a humid environment, the surface of copper absorbs moisture and forms a thin water film. The oxygen dissolved in this water film, along with the present electrolytes, creates an electrolytic solution that provides a medium for ionic conduction, enabling the flow of electric current between the anode and cathode. In this process, copper itself acts as the anode, while the cathode can be impurities on the copper surface, different metal phases, or certain components within the

electrolytic solution. This can lead to concentration polarization and follows the electrochemical corrosion mechanism. As a result, the oxidation rate of copper accelerates significantly. The typical reaction process is as follows:



Watanabe *et al.*³⁵ conducted an outdoor exposure experiment on copper (Cu) in Tokyo, testing for one month in both summer and winter. Subsequent analysis of the corrosion products revealed that in the summer, the primary products were cuprous oxide (Cu_2O) and basic copper sulfate ($\text{Cu}_4\text{SO}_4(\text{OH})_6 \cdot \text{H}_2\text{O}$). In contrast, only Cu_2O was generated in the winter. Additionally, the surface concentrations of sulfur (S) and chlorine (Cl) on the copper, as well as the thickness of the corrosion product layer, were lower in winter compared to summer. These differences are primarily attributed to variations in temperature and relative humidity (RH) between the two seasons, which affect the salt concentration in the thin liquid film on the copper surface.

In summary, forming a stable thin film on the copper surface that effectively isolates oxygen and water is crucial for enhancing its oxidation resistance.

Furthermore, in copper nanocrystals, the (110) and (100) crystallographic planes exhibit higher activity compared to other planes. These planes more readily adsorb oxygen to form Cu_2O nanoparticles, ultimately constructing a dense Cu_2O oxide

layer.^{36,37} Rough step edges on the copper powder surface play a pivotal role in oxygen adsorption, serving as primary sites for oxygen growth at surface steps. To minimize oxygen adsorption, it is essential to avoid such step edges. Consequently, the Cu (111) surface, characterized by a closely packed atomic arrangement, demonstrates significant advantages over other copper planes.³⁸ This is because single-atom step edges impose a high energy barrier against oxygen penetration. Additionally, when oxygen coverage on face-centered cubic (fcc) surface sites reaches 50%, further adsorption of oxygen atoms is suppressed.³⁹ Thus, the oxidation process of copper is fundamentally linked to its crystallographic orientation (Table 2).

The direct relationship between oxidation mechanisms and the rational design of modification strategies is summarized in the table below:

3. Modification method of nano-copper

Currently, the primary modification techniques for nano-copper include coating, core–shell structure construction, functional group modification, complexation modification, and coordination layer modification. These methods aim to enhance the oxidation resistance of nano-copper while improving its stability to varying degrees. The following sections will provide a comprehensive review of recent advancements in each of these technologies.

3.1. Coating

Coating involves the application of specific materials that interact physically or chemically with the copper surface to form a stable protective film, effectively isolating oxygen and water,

Table 2 The direct correlation between the five strategies and the oxidation mechanism

Strategy	Detailed elucidation
Coating	Forming a stable thin film on the copper surface that effectively isolates oxygen and water is crucial for enhancing its oxidation resistance
Core–shell structures	Core–shell structures represent a perfect embodiment of the Valensi–Carter mechanism. The core design principle involves using a complete and uniform shell material to entirely isolate the copper core from any environmental contact. An ideal shell should exhibit extremely low diffusion coefficients for both oxygen and metal ions, thereby minimizing the oxidation rate
Functional group modification	Specific functional groups, such as $-\text{SH}$ and $-\text{COOH}$, play a role that extends beyond merely improving dispersibility. They can engage in strong chemical interactions with the copper surface (<i>e.g.</i> , forming $\text{Cu}-\text{S}$ bonds), effectively passivating the highly active sites. This passivation layer alters the electronic structure at the interface and increases the activation energy of the oxidation reaction, directly countering the ion migration step described in the Cabrera–Mott mechanism
Complexation modification	The formation of a stable, inert complex layer between complexing agents and copper ions essentially constitutes chemical passivation. This stable layer consumes surface active sites available for oxidation reactions, resulting in a thermodynamically more stable interface. Consequently, it raises the energy barrier for initial oxidation, aligning with the Cabrera–Mott mechanism's description of interfacial reaction kinetics
Coordination layer modification	The coordination layer strategy demonstrates a concept of synergistic protection. The dense and well-ordered molecular film formed through strong coordination bonds not only provides an excellent physical diffusion barrier (Valensi–Carter mechanism) but also effectively passivates the copper surface <i>via</i> robust chemical bonding, modulating the interfacial potential (Cabrera–Mott mechanism). Thereby, it achieves dual effects of both physical and chemical protection



thereby inhibiting oxidation reactions. However, due to the ultra-small particle size, high specific surface area, and elevated surface energy of nano-copper, agglomeration is more likely to occur during the coating process. This makes coating operations inherently challenging, necessitating precise process control to ensure uniformity and integrity of the coating layer.

3.1.1. RGO/CuNWs. In recent years, graphene has been extensively utilized for surface modification and performance enhancement of copper nanowires (CuNWs) due to its distinctive two-dimensional structure and exceptional physicochemical properties, typically involving dual mechanisms of coating and supporting. Researchers have achieved synchronous reduction and composite formation between graphene oxide (GO) and copper precursors through strategies such as one-pot hydrothermal synthesis, electrostatic self-assembly, and co-reduction. For instance, Ye *et al.*⁴⁰ synthesized reduced graphene oxide/copper nanowire (RGO/CuNW) composites *via* a polyol-based one-step hydrothermal method, optimizing the RGO coating effectiveness by adjusting the ethylene glycol/glycerol ratio and GO concentration. Kim *et al.*⁴¹ employed hydrazine hydrate as a single reducing agent to simultaneously reduce GO and copper salts at low temperatures, producing Cu-RGO nanocomposites, but the use of toxic reagents limited its environmental friendliness. Zhou *et al.*⁴² adopted glucose as a green reductant to achieve *in situ* growth of CuNWs and nano-copper on RGO surfaces, forming an RGO/Cu/RGO sandwich structure that significantly improved the material's high-temperature oxidation resistance. These methods simplify the fabrication process through *in situ* reduction and structural design yet require precise control of reaction kinetics to prevent agglomeration of nano-copper and defect generation in graphene.

The performance of composite materials is highly dependent on the precise control of process parameters. For example, Hasan *et al.*⁴³ utilized electrospinning technology and the co-reduction effect of a PVP carbon source with a binary solvent to achieve *in situ* generation of nano-copper and reduced graphene oxide (RGO) during the electrospinning process. However, the effects of PVP content and annealing temperature on copper grain size and graphene crystallinity require strict optimization. In contrast, Navik *et al.*⁴⁴ employed supercritical CO₂ to exfoliate graphene nanosheets (GNs) and then used a hydrothermal method to enable the *in situ* growth of Cu nanowires (CuNWs) between GN layers (Fig. 3), forming a multi-layered protective structure. Nevertheless, achieving uniform dispersion of graphene remains a bottleneck for scalable fabrication. Meanwhile, Tseng *et al.*⁴⁵ adopted a chemical vapor deposition (CVD) approach to catalytically grow multilayer graphene (MLG) shells on nano-copper. While this method yields highly crystalline coatings, the high-temperature processes and equipment complexity result in significantly increased costs. These cases collectively demonstrate that the synergistic regulation of process parameters—such as reductant type, temperature, and pressure—is essential to balancing material performance with manufacturing feasibility.

Environmentally friendly fabrication technologies have emerged as a significant research focus in recent years. For

instance, Lin *et al.*⁴⁶ developed hydrogen-annealed reduced graphene oxide/copper nanowire (h-RGO/CuNW) films using glucose and lactic acid as reductants combined with hydrogen annealing. Their green synthesis process eliminates toxic reagents while leveraging the RGO layer to enhance the substrate adhesion and oxidation resistance of CuNWs. Similarly, Wang *et al.*⁴⁷ constructed a single-crystal graphene/copper nanowire network/UV-curable resin (SCG/CuNW/UVR) sandwich electrode *via* a layer-by-layer coating method, utilizing UV-curable resin for flexible encapsulation. This approach balances scalable production with performance stability. However, existing methods still face challenges, including the insufficient long-term stability of copper nanostructures and the limited availability of high-quality single-crystal copper substrates. Future research should focus on developing low-energy, low-cost continuous production processes and deciphering atomic-scale modulation mechanisms at the graphene/copper interface. Such advancements are critical to enabling the practical deployment of these composites in flexible electronics and energy storage devices.

3.1.2. Carbon modification strategies. Carbon materials, due to their high chemical stability and interfacial compatibility, have demonstrated significant value in the antioxidation enhancement and functionalization design of nano-copper. By employing techniques such as carbon encapsulation, *in situ* carbonization, and composite structure design, researchers have developed various green preparation methods for carbon-modified copper composite materials.

Carbon modification strategies primarily focus on the precise control of carbon source selection and the encapsulation structure. For instance, the team led by Huangqing Ye *et al.*⁴⁸ utilized biomass as a multifunctional reagent, serving as a reducing agent, capping agent, and template. They successfully synthesized two-dimensional dendrite-like Cu/C hybrid materials through a one-pot bio-hydrothermal method. In this process, hydrothermal carbonization achieved *in situ* encapsulation of graphite carbon, ensuring both green chemistry and scalability. Similarly, Xiulin Shu *et al.*⁴⁹ employed a sol-gel method combined with self-combustion and carbothermal reduction. Using γ -polyglutamic acid (γ -PGA) as a dispersant and Tween-80 as a reducing agent, they prepared amorphous carbon-coated nano-copper in an aqueous medium. The XRD (Fig. 4) and XPS (Fig. 5) results demonstrated the high antioxidant properties of zero-valent copper. These methods, through functionalization of carbon sources and design of reaction pathways, achieved uniform encapsulation of the carbon layer. However, they face challenges in scaling up for industrial production.

The performance of carbon encapsulation layers is closely related to process parameters. Myung Hyun Kang *et al.*⁵⁰ proposed an ultrasound-assisted carbonization strategy, forming a carbon layer encapsulating nano-copper(Cu/C) through the carbonization of organic matter in an argon atmosphere. The mild reaction conditions and short operation time of this method significantly surpass those of conventional high-temperature methods. However, the issue of nanoparticle aggregation after heat treatment still requires optimization



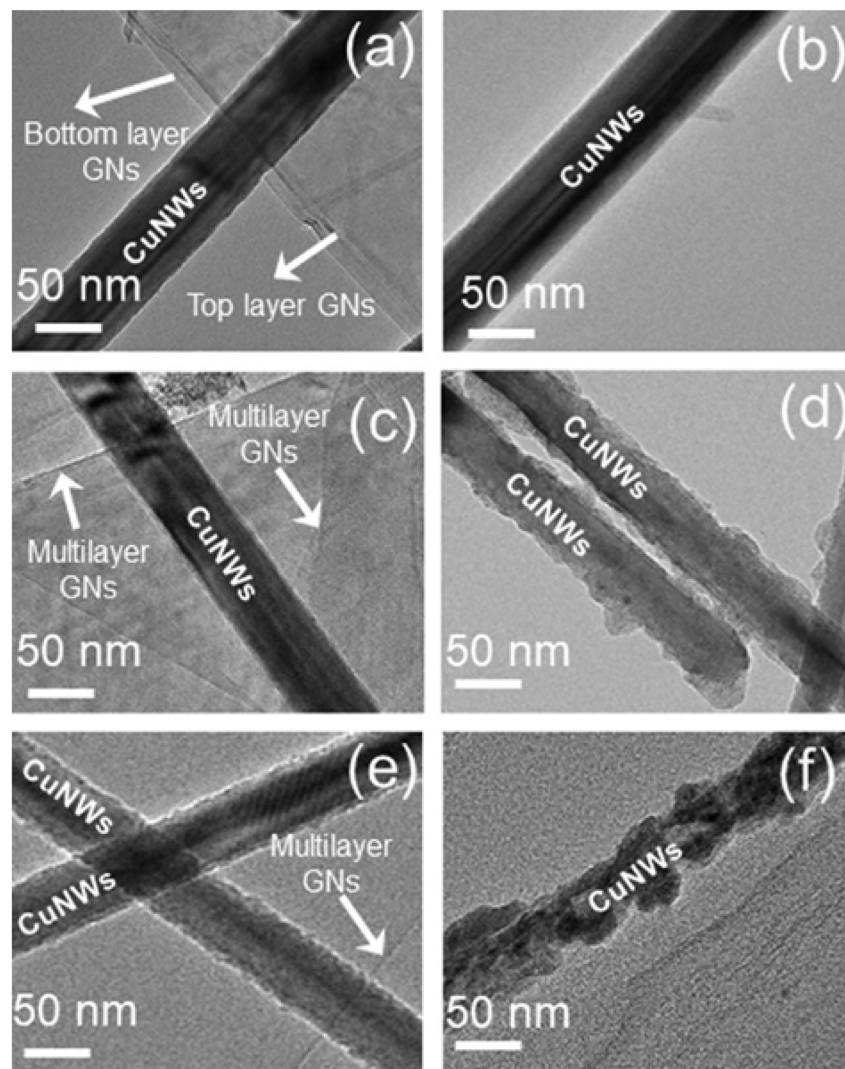


Fig. 3 TEM images of CuNWs with (a) and without GN protection (b) before the stability test; with (c) and without (d) GN protection after the test at 25 °C for 46 days and 4 days; with (e) and without (f) GN protection after the test at 60 °C for 46 days and 1 day.⁴⁴

through surface modification or dispersants. While the method by Shu *et al.*⁴⁹ aligns with the principles of green chemistry, the multi-step process involving sol-gel and carbothermal reduction increases process complexity and limits production efficiency. These examples highlight the need to co-optimize process parameters such as ultrasonic power, annealing temperature, and carbon source concentration to enhance the oxidation resistance and mechanical stability of the composite materials.

Current research focuses on developing low-toxic and efficient carbon modification technologies. Ye's bio-inspired hydrothermal method avoids the use of toxic reagents, and the two-dimensional dendritic structure endows the material with high surface area and active sites. Meanwhile, Kang's ultrasound-assisted method simplifies the process and reduces energy consumption, aligning with the requirements of sustainable manufacturing. However, existing technologies still face challenges such as insufficient uniformity of the carbon layers and limited long-term stability of the copper core. Future

research should further explore the application of novel bio-based carbon sources (*e.g.*, cellulose⁵¹ and chitosan⁵²), develop continuous production processes, and utilize molecular dynamics simulations to reveal the interaction mechanisms at the carbon-copper interface. These efforts aim to promote the practical application of carbon-modified copper-based composites in catalysis, flexible electronics, and other fields.

3.1.3. Other coatings. Beyond traditional graphene or carbon encapsulation, researchers have achieved precise control over the properties of CuNWs through innovative strategies such as surface passivation, multi-layer encapsulation, and low-temperature synthesis. However, different methods exhibit significant differences in terms of process complexity, environmental friendliness, and long-term stability.

The selection of surface passivation agents and the design of encapsulation structures directly affect the anti-oxidation capability of CuNWs. Research by Jian-Ming Chiu *et al.*⁵³ revealed that the traditional dispersant PVP may accelerate the oxidation of CuNW surfaces, while the use of a polyimide (CPI)



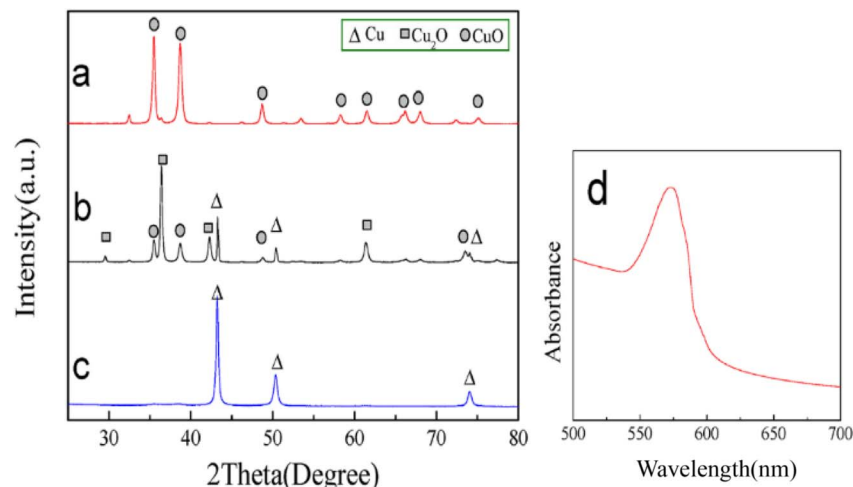


Fig. 4 X-ray diffraction spectra of C/Cu (a), C/Cu (b) and Cpt/Cu (c). The UV-Vis spectrum of Cpt/Cu (d).⁴⁹

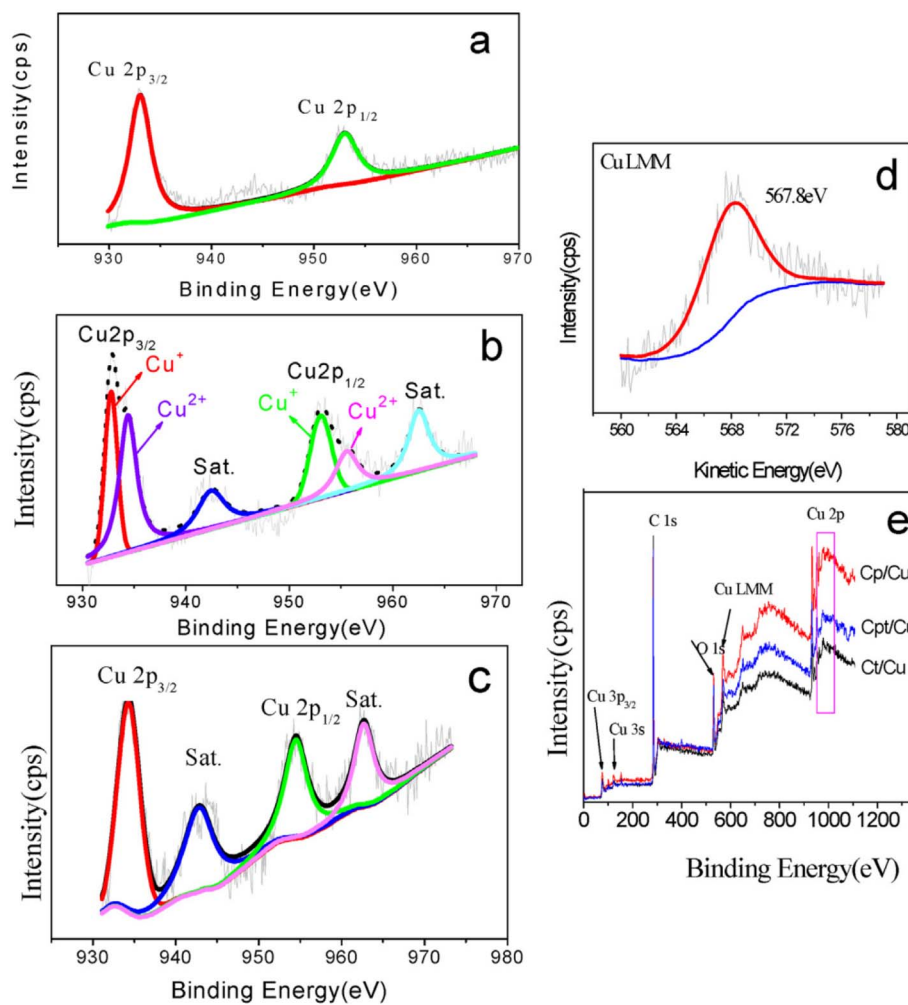


Fig. 5 Cu 2p_{3/2} and Cu 2p_{1/2} XPS spectra of Cpt/Cu (a), C/Cu (b) and C/Cu (c), the Cu LMM Auger transition energies of Cpt/Cu (d) and the survey spectrum (e) of the three C/Cu samples.⁴⁹

coating significantly reduces surface roughness and forms a dense protective layer, enabling CuNWs to remain stable for 90 days. However, long-term durability still requires further verification. Insic Hong *et al.*⁵⁴ proposed a multi-layer cooperative encapsulation structure of CuNW/PI/SiO_x (CuPS), where the interface optimization between polyimide (PI) and SiO_x provides the material with multi-faceted protection against high temperatures, humidity, and chemical corrosion. Such technologies enhance stability through physical-chemical synergistic effects, but complex encapsulation processes may limit their scalability for large-scale applications.

Environmentally friendly surface modification technologies remain a research hotspot. Suhyun Lee *et al.*⁵⁵ utilized food-grade dimethyl sulfoxide (DMSO) to achieve the green synthesis of silver-coated copper nanowires, avoiding the use of toxic reagents. Sevim Polat Genlik *et al.*⁵⁶ employed benzotriazole (BTA) passivation to form an anti-dissolution polymer membrane on the surface of CuNWs, offering a low-cost and straightforward process. Meanwhile, Jongyoun Kim *et al.*⁵⁷ developed a flash irradiation method to wrap CuNWs with two-dimensional quantum dots (QDs) under low-temperature, non-vacuum conditions, enhancing oxidation and mechanical stability through interfacial assembly of two-dimensional materials. However, this method relies heavily on specialized equipment. While these approaches reduce environmental risks, challenges such as the uniformity of the passivation layer and the long-term interfacial adhesion strength remain to be addressed.

3.2. Core-shell structures

Core-shell structures, through interfacial engineering and rational design of shell materials, enable synergistic enhancement of oxidation resistance, electrical conductivity, and mechanical stability in copper-based nanomaterials. Researchers have developed diverse core-shell systems based on various shell components (metallic, carbon-based, polymeric, ceramic, *etc.*) and fabrication techniques (*in situ* synthesis, electrodeposition, chemical vapor deposition, *etc.*). The critical design principles focus on achieving uniform shell encapsulation and robust interfacial coupling between the core and shell components. This architectural optimization fundamentally determines the comprehensive performance improvement of copper-based core-shell nanostructures.

The choice of shell components directly influences the performance orientation of core-shell structures. Metal shells, such as nickel (Ni) or silver (Ag), suppress copper oxidation through electronic shielding effects. For instance, Wanli Li *et al.*⁵⁸ developed copper@nickel core-shell ink, which forms highly conductive flexible electrodes after low-temperature annealing (Fig. 6). Similarly, Yuqing Xu *et al.*⁵⁹ utilized tannic acid chelation to prepare low-silver-content Cu@Ag particles, achieving excellent anti-oxidation properties while maintaining cost-effectiveness. On the other hand, non-metal shells enhance stability through physical isolation and chemical inertness. For example, Xiaojuan Li *et al.*⁶⁰ constructed a nano-copper@GO sandwich structure, where the graphene oxide (GO) layer inhibits copper oxidation and improves conductivity. Guozhen Liu *et al.*⁶¹ employed an LPCVD method to grow a hexagonal boron nitride (h-BN) shell (~5 nm thick) on the surface of CuNWs, leveraging its high thermal conductivity and insulating properties to expand the application of copper-based materials in high-temperature electronic devices. Such designs require precise control over shell crystallinity and interfacial adhesion strength to avoid cracking caused by stress mismatches.

The performance of core-shell structures is highly dependent on the precise control of process parameters. Electrochemical methods, such as Cu@Ni electrodeposition proposed by He Zhang *et al.*⁶², offer advantages in speed and cost-effectiveness but require optimization of current density and electrolyte composition to improve shell density. Solution reduction methods, like preparation of polypyrrole (PPy) (Cu@PPy) by Kun Liu *et al.*⁶³, achieve uniform polymer encapsulation through *in situ* polymerization but face challenges in product purification due to byproducts, which can affect yield. Advanced processes, such as multi-level modification of Cu@Ag@ZIF-8 by Zhi-Qiang Wang *et al.*⁶⁴, enhance chemical stability by incorporating a metal-organic framework (MOF) shell, though multi-step reactions increase process complexity. Additionally, hydrothermal synthesis of CuNWs@C performed by Xiaolan Tong *et al.*⁶⁵ requires precise control of the carbon layer growth dynamics (3–8 nm) to prevent conductivity loss caused by an overly thick layer. Yingcui Fang *et al.*⁶⁶ employed oxygen plasma irradiation (OPI) to construct a dense copper oxide (CuO) shell, resulting in a stable nano-copper@d-CuO core-shell structure with high stability for localized surface plasmon resonance (LSPR). These examples highlight the

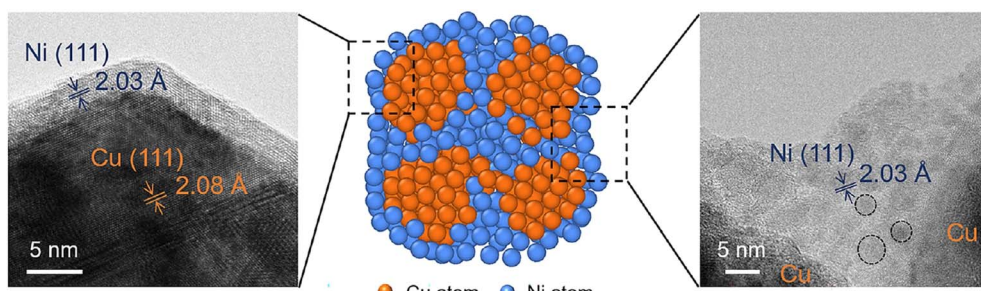


Fig. 6 Schematic and corresponding HR-TEM images of the *in situ*-formed Cu@Ni core–shell nanostructures.⁵⁸



challenges and opportunities in fabricating core–shell structures and emphasize that process simplification and the development of high-throughput fabrication techniques are crucial for large-scale applications.

Core–shell copper-based materials show great potential in flexible electronics, catalysis, and biomedical fields: for instance, the CuNW@G core–shell aerogel developed by Shiting Wu *et al.*⁶⁷ through its superhydrophobic design and PDMS encapsulation, achieved high sensitivity in pressure sensing. Similarly, the nano-copper@C nanocomposite materials created by Hai-feng Chen *et al.*⁶⁸ leveraged the antibacterial properties of the carbon shell to explore biomedical applications. However, current technologies still face challenges such as insufficient uniformity of the shell layer (*e.g.*, SnO₂–Cu NWs prepared by Le Zhao *et al.*⁶⁹) and the use of toxic reagents (*e.g.*, AlF₃ treatment for Al₂O₃ shells).

Core–shell modification, achieved through multiscale interface design and process innovation, has significantly enhanced the comprehensive performance of copper-based materials. Overcoming challenges such as shell layer uniformity control, developing environmentally friendly processes, and optimizing long-term stability will be the core pathways to transitioning these materials from laboratory research to industrial applications.

3.3. Functional group modification

Functional groups, through their chemical activity and interfacial interactions, provide molecular-level control for

optimizing the performance of copper-based nanomaterials. Based on the varying reducing properties, coordination capabilities, and steric hindrance effects of different functional groups, researchers have developed diversified surface modification strategies. The core of these strategies lies in achieving oriented binding of functional groups to the copper surface and their functional synergy.

Functional groups with reducing capabilities, such as –OH and –NH₂, can participate in the reduction of copper precursors, enabling precise control over the nucleation and growth of nanostructures. Rahul Navik *et al.*⁷⁰ utilized the –OH groups in graphene oxide derivatives (Goh) to adsorb Cu²⁺ ions through dipole–ionic interactions and gradually reduce them to metallic copper, promoting the directed growth of copper nanowires (CuNWs). Additionally, the surface anchoring effect of the –OH groups enhanced the stability of the resulting composite materials. Similarly, Zhou Hongfeng *et al.*⁷¹ employed chitosan as a multifunctional template, where the –NH₂ and –OH groups in its molecular structure formed stable coordination complexes with Cu²⁺ (Fig. 7). After reduction with hydrazine, uniformly dispersed CS–Cu nanoparticles (CS–nano–copper) were obtained. The functional group network within chitosan effectively suppressed the oxidation and aggregation of nano–copper. These methods leverage the dual functionality of functional groups (as reducing agents and stabilizers) to simplify the synthesis process. However, precise control over pH and functional group density is required to balance reduction kinetics with structural stability.

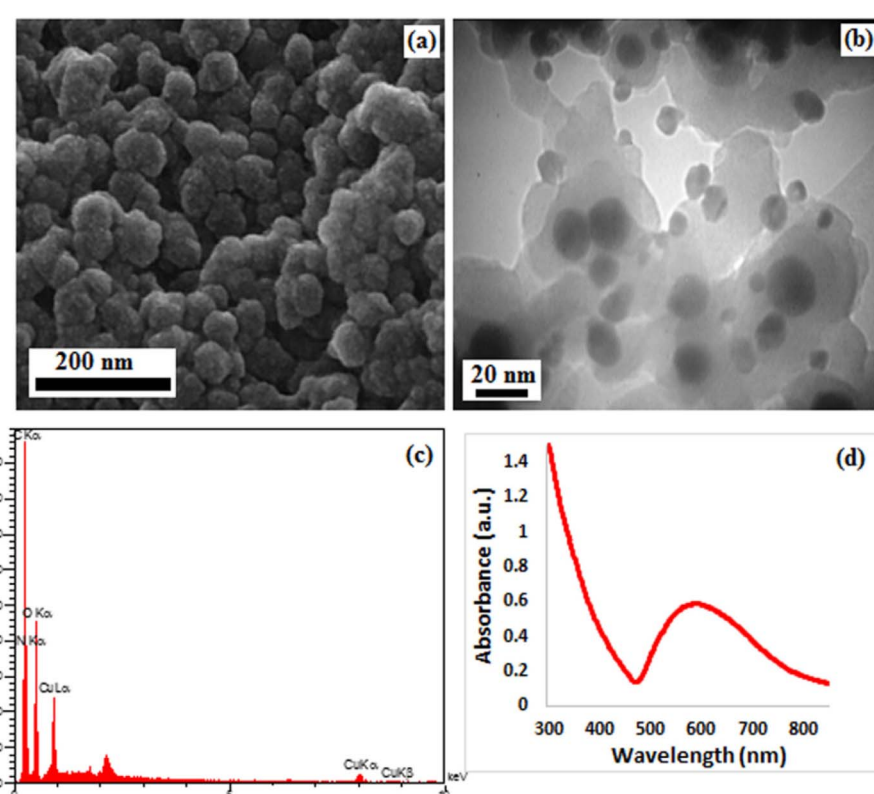


Fig. 7 (a) FESEM and (b) TEM images of CS–Cu NPs with (c) their EDX pattern and (d) UV–Vis spectrum.⁷¹



Specific functional groups, such as $-SH$ and $-COOH$, play a crucial role in enhancing the dispersion and environmental stability of nano-copper through mechanisms like electrostatic repulsion or chemical passivation. Zhongmin Yin *et al.*⁷² demonstrated this by modifying CuNWs with 2-mercaptoethanol, which contains both $-SH$ and $-OH$ groups. The $-SH$ group forms strong covalent bonds with the copper surface, imparting negative charges to the nanowires and achieving high-concentration stable dispersion through electrostatic repulsion. Additionally, the physical barrier effect of the functional groups significantly reduces the contact probability between oxygen molecules and the copper surface, thereby slowing down the oxidation process. Similarly, Ricardo J. B. Pinto *et al.*⁷³ extracted a natural reducing agent rich in phenolic $-OH$ and $-COOH$ groups from blue eucalyptus bark. These functional groups form a dense adsorbed layer on the CuNW surface through chelation, effectively stabilizing copper atoms and neutralizing free radicals. This innovation allows the CuNWs to maintain their anti-oxidation stability in air for up to 30 days. Lulu Tian *et al.*⁷⁴ took a different approach by *in situ* grafting amine ($-NH_2$) and carboxyl ($-COOH$) groups onto nano-copper using ligand interactions. This method resulted in amine-carboxyl co-modified nano-copper(Cu-AC) that exhibits excellent anti-oxidation, dispersion, and antibacterial properties. These strategies leverage the multi-interfacial effects of functional groups to enhance material performance. However, it is crucial to avoid excessive modification, which could lead to a loss of conductivity in the nano-copper.

Additionally, Shi-Yu Xia *et al.*⁷⁵ proposed a novel method for synthesizing end-capped oleylamine (OAM) ligand-modified Cu nanoparticles. In this method, the long alkyl chains (C_nH_{2n-1}) and amine groups (NH_2) in the OAM molecules play crucial roles during the air-annealing process: when the temperature exceeds 175 °C, the OAM decomposes. The long alkyl chains are oxidized between 175 °C and 235 °C, producing carbon dioxide and water, which consume oxygen and form an inert protective atmosphere, thereby inhibiting the oxidation of nano-copper. The OAM-capped Cu nanoparticles exhibit self-reducing capabilities, enhancing their anti-oxidation properties.⁷⁶

The introduction of functional groups not only improves the anti-oxidation performance of nano-copper but also enhances its

dispersion in polymer matrices. Certain functional groups can even impart additional exceptional properties to nano-copper, expanding its application domains. However, not all functional groups can effectively enhance the anti-oxidation capabilities of nano-copper. Extensive experimentation and research are required to screen and select suitable functional groups. Generally, the modification processes are relatively complex, which increases the difficulty of functional group selection.

3.4. Complexation modification of nano-copper

Complexation modification is a sophisticated technique employed to enhance and tailor the properties of nano-copper. This method leverages the principles of coordination chemistry, where specifically designed ligands interact with the surface atoms or ions of nano-copper to form stable complexes. The formation of these complexes allows for the optimization and precise control of the nanoparticles' characteristics, such as stability, solubility, and reactivity, making them suitable for a wide range of applications, including catalysis, electronics, and optics.⁷⁷

The chemical structure of ligands and reaction conditions directly influence the efficiency of complex formation and the resulting properties of the complex. Shun Yokoyama *et al.*⁷⁸ used citric acid (CA) as a chelating agent under pH 3.0 conditions, achieving rapid removal of surface oxides from Cu NPs and forming stable surface complexes within a short reaction time (5 minutes). The carboxyl ($-COOH$) and hydroxyl ($-OH$) groups in citric acid formed multi-dentate coordination bonds with the copper surface, significantly inhibiting the oxidation process (Fig. 8 and 9). Nasir Sarwar *et al.*⁷⁹ modified nano-copper with citric acid and blended them with sodium alginate paste. Through low-temperature sintering, they induced interfacial cross-linking between the complex and the polymer, enhancing the material's mechanical strength and conductivity. However, the thermal decomposition of ligands during sintering could lead to carbon residues, necessitating inert atmosphere protection or gradient heating to avoid impurities. Yu-Mei Wang *et al.*⁸⁰ further designed flexible bipyrazole ligands (H_2L1), which reacted with $Cu(OH)_2$ under solvent thermal conditions to generate octanuclear copper nanoclusters (Cu_8). The ligands were converted *in situ* into their deprotonated forms ($L2/L3$), with the

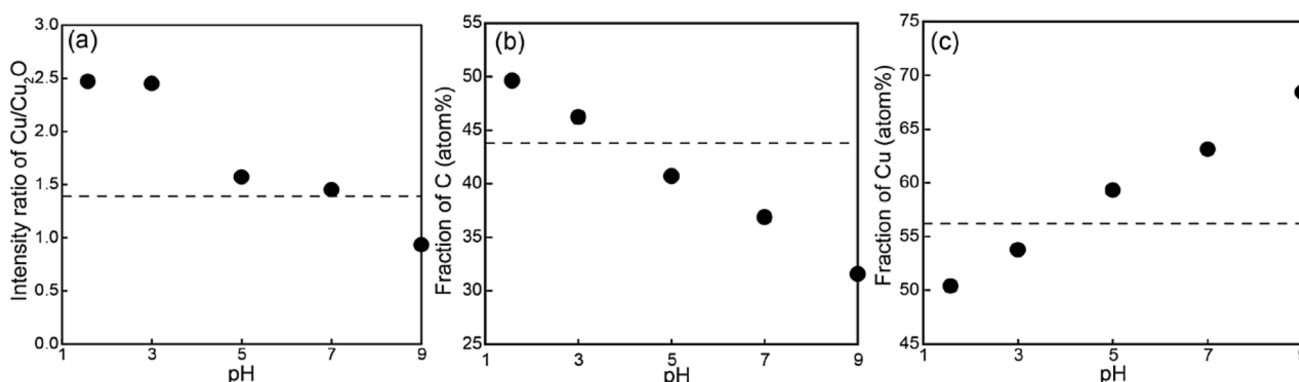


Fig. 8 (a) Intensity ratio of Cu/(Cu₂O) and fractions of (b) C and (c) Cu calculated from XPS and Auger profiles of the Cu NPs after treating them at various pH values for 30 min. Dashed lines indicate values for untreated Cu NPs.⁷⁸



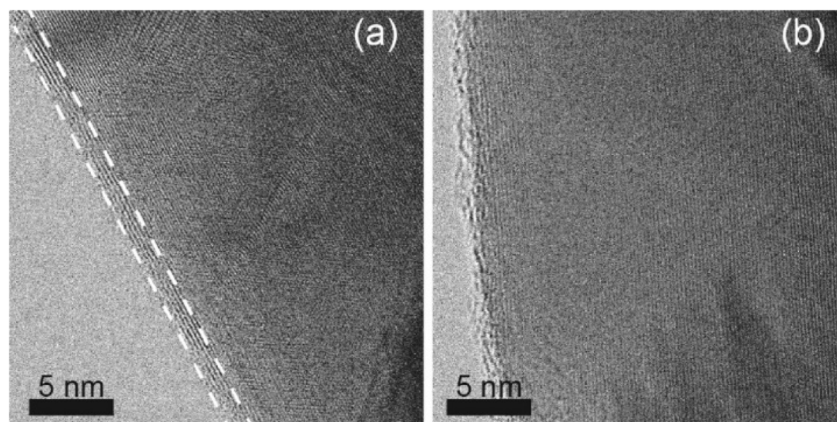


Fig. 9 STEM micrographs of Cu NPs in TE mode (a) before and (b) after the treatment. The white dashed lines show the region of the (200) cubic plane (Cu_2O).⁷⁸

nitrogen atoms in the bipyrazole rings forming strong coordination bonds with copper ions, thereby tuning the electronic structure and stability of the nanoclusters. These methods achieve controlled synthesis of copper nanostructures by precisely matching the functional groups of ligands with reaction kinetics, though excessive complexation must be avoided to prevent surface passivation. Arnau Oliva-Puigdomènec *et al.*⁸¹ found that the anti-oxidation mechanism of nano-copper primarily relies on the interaction between surface ligands (*e.g.*, carboxylic acids) and copper surface oxides, forming a protective layer that reduces oxygen contact and enhances surface passivation through ligand dissociative adsorption.

The application of natural ligands provides an environmentally friendly solution for modifying nano-copper. Muhammad Imran Din *et al.*⁸² utilized plant extracts containing flavonoids and other compounds, where the carbonyl groups and π -electron systems stabilize nano-copper through chelation. Additionally, the antioxidant properties of plant polyphenols synergistically enhance the material's durability. Priyanka Sharma *et al.*⁸³ demonstrated that the thiol group ($-\text{SH}$) in cysteine dynamically interacts with copper ions to form redox-active complexes, which inhibit copper-catalyzed free radical chain reactions (*e.g.*, Fenton reactions), reducing oxidative stress. Furthermore, the regenerative cycling mechanism of cysteine extends the anti-oxidation duration. While these bio-inspired strategies are green and efficient, the complexity of plant extract components may introduce uncontrollable variables, necessitating standardized extraction processes to improve modification consistency.

Complexation modification offers significant advantages in enhancing the anti-oxidation properties of nano-copper, such as effectively suppressing oxidation, achieving good dispersion and stability, and offering high cost-effectiveness. However, it may sometimes introduce impurities.

3.5. Coordination layer modification of nano-copper

The modification of nano-copper through coordination layers fundamentally relies on coordination chemistry principles. By

utilizing specific ligands to form coordination bonds with the surface atoms or ions of nano-copper, a specialized coordination layer is constructed on the surface of nano-copper. This process enables precise control and optimization of the properties of nano-copper.

The electronic structure and functional group properties of the ligands determine the stability and protective effectiveness of the coordination layer. Peng Zhang *et al.*⁸⁴ synthesized a high-precision, highly conductive, and oxidation-resistant nano-copper ink. This was achieved by utilizing the interactions between isopropylamine (IPA) and copper ions and nanoparticles. IPA molecules contain amino ($-\text{NH}_2$) and hydroxyl ($-\text{OH}$) groups, and the nitrogen (N) and oxygen (O) atoms in these groups can provide lone pair electrons. During the synthesis process, Cu^{2+} ions in copper acetate have vacant orbitals, allowing them to form coordination bonds with IPA molecules and generate Cu^{2+} -IPA complexes (Fig. 10). When Cu^{2+} is reduced to Cu, the outermost electron layer of the nano-copper still has vacant orbitals, enabling IPA to adsorb onto its surface. This adsorption effectively suppresses the aggregation and oxidation of nano-copper in air. The IPA layer acts as a barrier, preventing oxygen from coming into contact with the nano-copper and reducing oxidation reactions. Additionally, it avoids particle aggregation caused by high surface energy.⁸⁴ Similarly, Yu Zhang *et al.*⁸⁵ utilized the conjugated double bonds and hydroxyl groups of L-ascorbic acid in a polyol method to achieve *in situ* reduction and coordination passivation of Cu^{2+} . The resulting nano-copper remained unoxidized in air for 30 days. This design employs a reduction-coordination dual-function mechanism of ligands to simplify the process. However, it requires balancing the ligand concentration and reaction dynamics to avoid over-passivation, which could block active sites.

Dynamic coordination strategies enhance the environmental adaptability of protective layers through multi-ligand synergy or interface reconstruction. Shuqing Hong *et al.*⁸⁶ combined formate (FA) and dodecanethiol (DT) for surface treatment of plate-like copper powder. FA forms a chemical passivation layer through coordination with the copper surface *via* its carboxyl



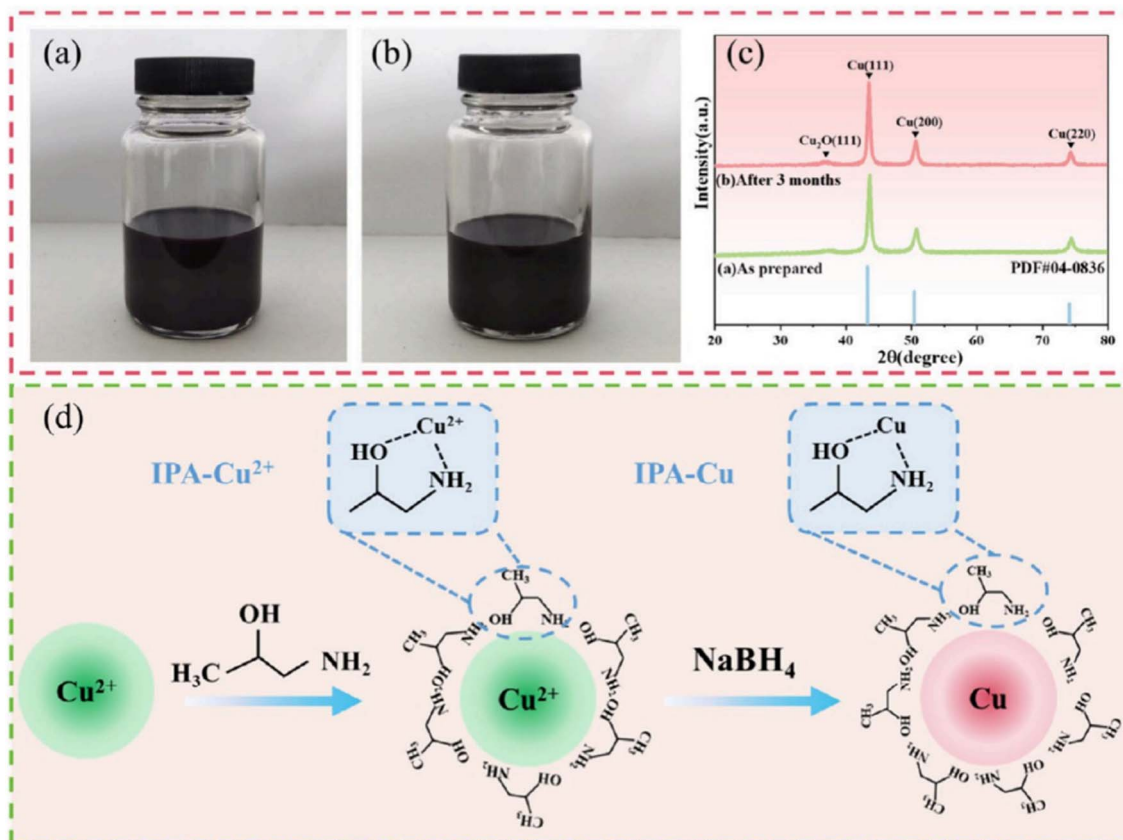


Fig. 10 Stability, oxidation resistance, and the formation mechanism of nano-copper. (a and b) Dispersions before and after three months of storage, (c) XRD patterns of nano-copper before and after three months of storage, and (d) schematic illustration of the mechanism for preparing nano-copper using reduced copper Cu^{2+} -IPA complexes.⁸⁴

group, while DT provides a hydrophobic barrier through its thiol ($-\text{SH}$) group. The synergistic effects of FA and DT ensure that the copper powder maintains its conductivity even after corrosion in 0.1 M NaOH solution. Similarly, Zhang *et al.*⁸⁷ utilized the catechol and amine groups of polydopamine (PDA) to form a redox-active coating on the surface of CuNWs. This coating is achieved through a dynamic coordination-polymerization mechanism, enabling long-term oxidation resistance. However, research by Qixuan Xiang *et al.*⁸⁸ revealed that formate (FA) passivation layers, assisted by oleylamine, preferentially form on the $\{100\}$ crystal facets of CuNWs. The intensity of the coordination bonds is influenced by crystallographic orientation, requiring precise control of the passivation layer uniformity through solvent thermal conditions. While these methods have improved material stability, the insufficient thermal or chemical stability of the ligands may lead to failure of the protective layer, necessitating further optimization of ligand anchoring strategies (Fig. 11).

Additionally, Huawei Li *et al.*⁸⁹ introduced ultrathin two-dimensional porous holmium oxide (Ho_2O_3) nanosheets into nano-copper to prepare ($\text{Cu}/\text{Ho}_2\text{O}_3$) composite catalysts, achieving modification of nano-copper. The unsaturated coordination sites of the holmium oxide nanosheets formed coordination bonds with the nano-copper particles, effectively

inhibiting the aggregation and structural changes of nano-copper during the reaction process, thereby enhancing its stability. However, the limitations of rare-earth resources and reaction conditions increase the difficulty and cost of practical applications.

This modification method can be applied to nano-copper materials of various shapes and sizes, such as nanowires and nanoparticles, demonstrating broad applicability. Nevertheless, some ligands may lack stability during the binding process with nano-copper, easily detaching during the reaction or usage, which could lead to a decline in the antioxidant performance of nano-copper. Furthermore, certain ligands may possess inherent toxicity, potentially posing threats to environmental and human health during application.

3.6. Others

Research on the mechanism by which ethylenediamine (EDA) regulates the antioxidant performance of nano-copper has revealed that its adsorption behavior on different crystal faces significantly influences the protective efficiency. According to theoretical calculations by Zihao Chen *et al.*⁹⁰ EDA exhibits differential adsorption on copper surfaces, with stronger binding energy on the Cu (100) face compared to the Cu (111) face. By calculating the energy barrier for water molecules penetrating the



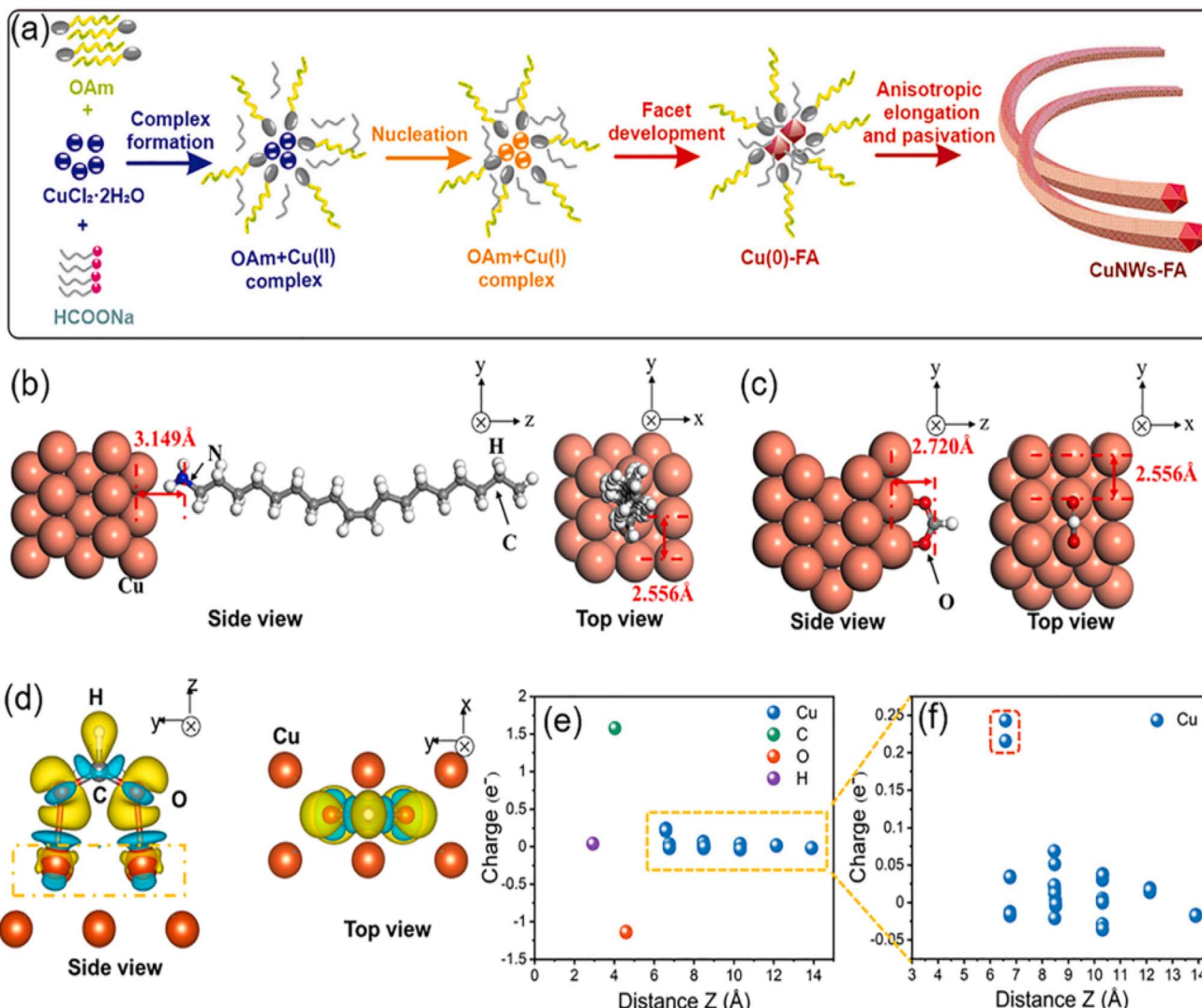


Fig. 11 CuNWs-FA forming mechanism and theoretical calculations. (a) Graphical representation of the CuNWs-FA formation mechanism. Optimized atomic configuration of (b) OAm and (c) FA adsorbed on the Cu [100] surface. (d) Electron charge density isosurface ($0.002 \text{ e } \text{\AA}^{-3}$) of FA adsorbed on the Cu [100] plane. Charge distribution of (e) total atoms and (f) Cu atoms at different Z distances.⁸⁸

EDA layer to approach the copper surface, it was found that the EDA layer on the Cu (111) surface, due to its higher atomic density, forms a more compact barrier. This results in a higher energy barrier (0.96 eV) for water molecule diffusion, providing superior oxidation protection for copper. In contrast, the energy barrier on the Cu (100) surface is lower (0.22 eV), leading to a relatively faster oxidation rate. These findings suggest that adjusting the coverage of EDA on copper surfaces, particularly increasing the coverage density on easily oxidized crystal faces such as Cu (100) (Fig. 12), could enhance the overall anti-oxidation performance of nano-copper. However, further research is still required to precisely control the adsorption and coverage of EDA on different crystal faces during actual preparation to fully leverage its antioxidant effects.

Amino acids and their derivatives have demonstrated significant potential in enhancing the antioxidant performance of nano-copper. Theoretical calculations indicate that amino acids

containing multiple functional groups, such as glutaramide and cysteine, form chemical bonds with the copper surface through O, S, and N atoms. The adsorption energy and corrosion inhibition efficiency are positively correlated (GLT > CYS > GLY), and a smaller energy gap (ΔE_{gap}) corresponds to higher reactivity.^{91,92} Experimental studies further confirm that L-arginine (L-Arg), due to the presence of an additional $-\text{NH}_2$ group, exhibits an 18% increase in adsorption energy compared to L-valine (L-Val), achieving a corrosion inhibition efficiency of 92% in a sulfuric acid medium.⁹² Additionally, functionalized carbon dots (N-CDs), through a synergistic effect of chemical adsorption *via* carboxyl/amine groups and physical adsorption *via* van der Waals forces, form a dense protective film on the copper surface. This results in an inhibition efficiency as high as 98.5%, while the thiol groups can dynamically repair defects in the oxidized layer.⁹³ These studies, ranging from molecular design to interface engineering, provide both theoretical and experimental evidence



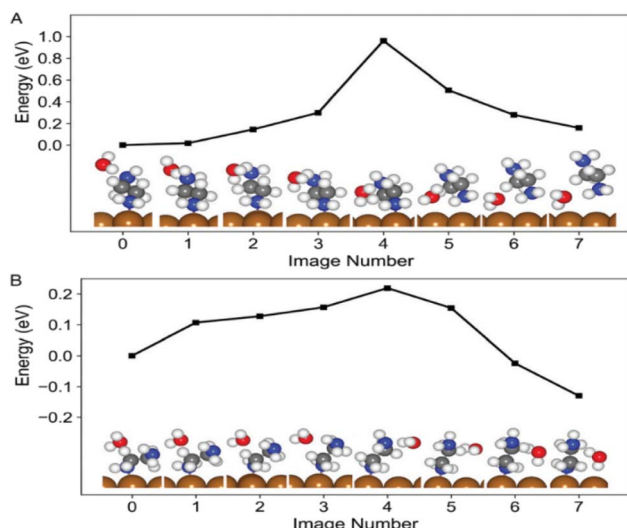


Fig. 12 Minimum-energy pathways for a water molecule to transit through EDA with 0.25 ML coverage on (A) Cu (111) and (B) Cu (100). Energies are relative to the energy of image 0. The insets show snapshots of the EDA and water for all states (image number) along the pathways (brown: Cu, blue: N, gray: C, and white: H).⁹⁰

for the development of efficient and environmentally friendly antioxidant technologies for nano-copper.

In the field of developing novel antioxidant systems, nano-copper based on two-dimensional $[\text{Ca}_2\text{N}]^+ \cdot \text{e}^-$ electron compounds has demonstrated significant advantages. Sung Su Han *et al.*⁹⁴ revealed that due to the substantial work function difference between the electron compound and nano-copper, pronounced charge transfer occurs from the electron compound to the nano-copper. This process results in the accumulation of transferred electrons on the surface of the nano-copper, rendering its surface negatively charged. This negative surface charge not only endows the nano-copper with abundant catalytically active sites but also significantly enhances its antioxidant performance. However, the high preparation cost of this method limits its

widespread application. In another study, J. E. Graves *et al.*⁹⁵ developed a (3-aminopropyl) trimethoxysilane (APTMS)-capped copper-methanol nanofluid, which exhibits superior dispersion stability and antioxidant properties compared to untreated bare copper nanopowder. This achievement fills the previous research gap regarding capped copper nanopowder/methanol solution studies. APTMS molecules can firmly adsorb onto the surface of nano-copper, forming an effective physical barrier layer that prevents the oxidation of nano-copper. However, it remains unclear whether the amine or silane group in the APTMS molecule interacts with the nano-copper, and the preparation conditions for this method are relatively harsh. Juncheng Qi *et al.*⁹⁶ proposed a novel antioxidant strategy utilizing ultra-small nanobubbles (NBs) to inhibit the oxidation of metallic copper in aqueous solutions, while elucidating the underlying reaction mechanisms. This work provides theoretical support and technical references for copper-based materials in various applications. The study identifies the interface-induced spatially separated redox reaction mechanism as the key factor. Under the influence of the nanobubble interfacial electric field, hydroxide ions (OH^-) dissociate into hydroxyl radicals ($\cdot\text{OH}$) and electrons (e_h^-). The $\cdot\text{OH}$ radicals accumulate at the interface and, when approaching the copper foil, oxidatively etch the copper surface, forming nanovoids and generating copper ions. Simultaneously, the electrons (e_h^-) enter the bulk water and react with copper ions, reducing them to metallic copper clusters (Fig. 13). Due to their high concentration and large specific surface area, ultra-small nanobubbles exhibit significant antioxidant effects, offering a new perspective for antioxidant research on nano-copper.

4. Challenges for industrial applications

While this review has focused on the comparative technical merits of various antioxidative strategies (as synthesized in Table 3), bridging the gap between laboratory innovation and industrial deployment remains a critical challenge. The path to commercialization is not solely determined by antioxidant

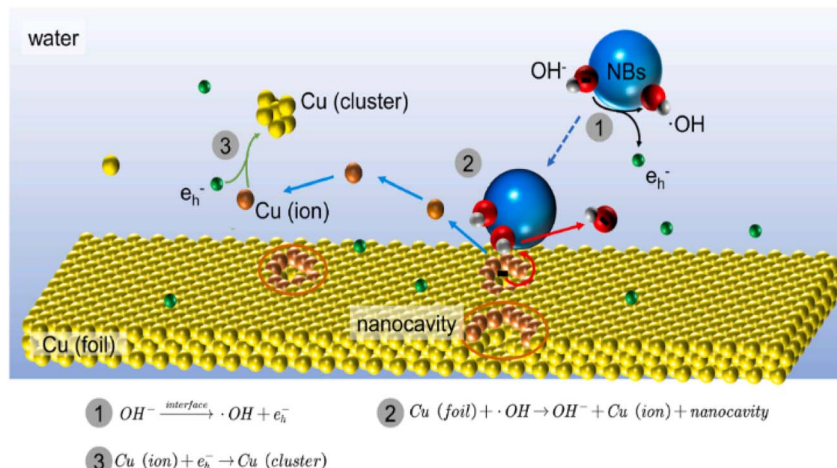


Fig. 13 Possible protective mechanism of metallic Cu in ultra-small NBs.⁹⁶



Table 3 Advantages, disadvantages, and future challenges of various strategies

Strategy	Advantages	Disadvantages	Future challenges
Coating	Most mainstream coating processes can utilize non-toxic and renewable raw materials, reducing hazards to the environment and operators	Due to the ultra-small particle size, high specific surface area, and elevated surface energy of nano-copper, agglomeration is more likely to occur during the coating process	Future efforts should focus on process optimization (e.g., simplifying steps and reducing equipment dependency) and developing new coating materials (e.g., highly stable two-dimensional materials)
Core–shell structures	The tunability of shell materials and structural parameters allows core–shell structures to be tailored to meet diverse application requirements	The preparation of most core–shell structures requires precise control of process parameters; some methods rely on complex equipment or multi-step procedures, limiting industrial application	First, developing precise coating techniques like atomic layer deposition (ALD) to address shell uniformity; second, optimizing green processes (e.g., using non-toxic reagents and simplifying procedures) to reduce scaling costs
Functional group modification	Balances oxidation resistance, dispersibility, and functional extensibility and can incorporate natural raw materials and mild processes	Screening for effective functional groups is challenging, and scaling up can be costly	Future efforts should focus on the extensive screening of suitable functional group types
Complexation modification	Effectively addresses oxidation and agglomeration issues and is adaptable to various needs in fields like conductivity, catalysis, and biology	Complexation conditions are sensitive and can easily introduce impurities	Separation and purification processes (e.g., ultrafiltration and gradient centrifugation) should be optimized to reduce impurity residues
Coordination layer modification	This modification method is applicable to nano-copper materials of various shapes and sizes (e.g., nanowires and nanoparticles), demonstrating broad applicability	The binding of some ligands lacks stability, making them prone to detachment during reactions or use, which reduces the oxidation resistance of nano-copper. Additionally, certain ligands may exhibit inherent toxicity, posing potential risks to the environment and human health	Future work should focus on developing new ligands with “strong coordination–high stability” (e.g., ligands featuring bidentate/tridentate functional groups) to enhance binding strength and promote the use of green, low-toxicity ligands (e.g., multifunctional molecules derived from natural plant extracts)

efficiency but is equally governed by factors of scalability, cost-effectiveness, environmental compatibility, and integration with existing manufacturing processes. Therefore, future research should not only aim for higher performance in controlled lab environments but also embrace a ‘design-for-manufacturability’ philosophy. This includes developing water-based, greener synthesis routes, adapting batch processes to continuous flow production, and conducting pilot-scale trials in collaboration with industry partners. We hope that this review provides a foundational framework that aids researchers in not only selecting scientifically intriguing strategies but also in prioritizing those with the greatest potential for real-world impact.

5. Conclusion and prospects

Nano-copper, with its excellent conductivity, flexibility, and cost-effectiveness, has demonstrated remarkable potential in flexible electronics, catalysis, and energy devices. Recent advancements in interfacial engineering—such as graphene and carbon encapsulation, core–shell structures, functional group modification, complexation, and coordination layer

design—have significantly enhanced its antioxidative properties, dispersion stability, and functional versatility. Graphene and carbon-based coatings leverage physical isolation and chemical inertness to mitigate oxidation, though challenges persist in achieving uniform graphene dispersion and simplifying complex fabrication processes. Core–shell architectures enable synergistic performance through multi-scale interfacial design, yet limitations in shell-layer uniformity and scalable synthesis hinder widespread adoption. Functional group and coordination layer modifications offer molecular-level control over surface passivation but require further optimization in long-term stability and environmental compatibility. Complexation strategies balance performance and simplicity *via* dynamic chelation mechanisms, though issues related to ligand selection and thermal stability demand resolution. Collectively, while interdisciplinary innovations have driven progress, critical gaps remain in material uniformity, process economics, and eco-friendly scalability.

Looking ahead, the evolution of materials science and technology is poised to yield more efficient, sustainable, and cost-effective antioxidative surface modification techniques for nano-copper. Such advancements will unlock its broader



application in high-end sectors, including advanced electronic devices, high-performance aerospace engines, and deep-sea exploration systems. Further mechanistic studies on anti-oxidative surface interactions will deepen theoretical understanding, guiding the design of next-generation copper-based nanomaterials. Innovations such as self-healing coatings and crystallographic orientation-specific passivation are required for addressing current limitations. Additionally, scalable manufacturing methods, such as atomic layer deposition⁹⁷ (ALD) and green synthesis routes, will bridge the gap between laboratory breakthroughs and industrial deployment.

By integrating fundamental insights with engineering ingenuity, nano-copper can transcend existing barriers, enabling transformative advancements in flexible electronics, energy storage, and biomedical technologies. Collaborative efforts across disciplines will be essential to harmonize performance, sustainability, and scalability, ultimately realizing the full potential of nano-copper in cutting-edge applications.

Author contributions

The manuscript was written through the contributions of all authors. All authors have given approval to the final version of the manuscript.

Conflicts of interest

The authors declare no competing financial interest.

Data availability

The data supporting this article have been included as part of the main manuscript text.

Acknowledgements

This work was supported by the Provincial Special Project of Chenzhou National Sustainable Development Agenda Innovation Demonstration Zone Construction (No. 2022SFQ44) and Zhuzhou City Mass Entrepreneurship and Innovation Elite Talent Program.

References

- 1 H. Gleiter, *Acta Mater.*, 2000, **48**, 1–29.
- 2 Z. Liang, N. T. Magar, R. K. Koju, I. Chessler, J. Zimmerman, Y. Mishin and E. Rabkin, *Acta Mater.*, 2024, **276**, 120101.
- 3 N. Yumeng, L. Yijian, Z. Binyuan, Z. Na and T. Qingbiao, *J. Funct. Mater.*, 2018, **49**.
- 4 J. Qin, C. Zhou, D. Wang, X. Li, T. Hu, J. Wang and Y. Yang, *J. Mater. Res. Technol.*, 2023, **25**, 773–785.
- 5 W. Yiqi, H. Fang, T. Zhongqiu, H. Luqi, C. Ge and G. Biao, *Copper Eng.*, 2024, 40–62.
- 6 L. Y. Chen, J. S. Yu, T. Fujita and M. W. Chen, *Adv. Funct. Mater.*, 2009, **19**, 1221–1226.
- 7 X. Zeng, P. He, M. Hu, W. Zhao, H. Chen, L. Liu, J. Sun and J. Yang, *Nanoscale*, 2022, **14**, 16003–16032.
- 8 C. Yin, Q. Li, J. Zheng, Y. Ni, H. Wu, A.-L. Kjønnsken, C. Liu, Y. Lei and Y. Zhang, *Adv. Powder Mater.*, 2022, **1**, 100055.
- 9 P. Deka, B. J. Borah, H. Saikia and P. Bharali, *Chem. Rec.*, 2019, **19**, 462–473.
- 10 J. Ramos-Zúñiga, N. Bruna and J. M. Pérez-Donoso, *Int. J. Mol. Sci.*, 2023, **24**, 10503.
- 11 M. J. Woźniak-Budych, K. Staszak and M. Staszak, *Molecules*, 2023, **28**, 6687.
- 12 Z. Guo, M. Li, B. Li, J. Jin and Y. Gao, *Arab. J. Chem.*, 2023, **16**, 105252.
- 13 S. Aghajani, A. Accardo and M. Tichem, *ACS Appl. Energy Mater.*, 2020, **3**, 5665–5675.
- 14 A. Mao, M. Ding, X. Jin, X. Gu, C. Cai, C. Xin and T. Zhang, *J. Mol. Struct.*, 2015, **1079**, 396–401.
- 15 S. T. Nataraja, R. Vishnu, E. V. Anoop, A. M. Chathoth, J. Valasseri and S. Babu, *ACS Appl. Nano Mater.*, 2025, **8**(10), 4946–4957.
- 16 J. Yang, J. Chen, Y. Zhou and K. Wu, *Sens. Actuators, B*, 2011, **153**, 78–82.
- 17 J.-H. Li, J.-X. Tang, L. Wei, S.-J. He, L.-q. Ma, W.-C. Shen, F.-Y. Kang and Z.-H. Huang, *N. Carbon Mater.*, 2020, **35**, 410–419.
- 18 W.-C. Chen, J.-G. Cheng, H.-P. Chen, N.-M. Ye, B.-Z. Wei, L.-M. Luo and Y.-C. Wu, *Trans. Nonferrous Metals Soc. China*, 2018, **28**, 1186–1191.
- 19 H. Yin, X. Zhang, Z. Guo, Y. Xu, X. Rao and C. Yuan, *Tribol. Int.*, 2023, **178**, 108085.
- 20 D. Yakang and W. Bingyan, *Mod. Archit. Electr.*, 2013, 63–68.
- 21 Z. Rui-qing, Z. Y.-. hong and L. Jing-mo, *J. Mech. Res. & App.*, 2014, **27**, 187–189.
- 22 K. Morshed-Bebehani, A. Aliyu, D. P. Bishop and A. Nasiri, *Mater. Today Commun.*, 2024, **38**, 108395.
- 23 W. Juanjuan, Y. Yingfeng, J. Hua, L. Licheng and X. Zixi, *China Adhes.*, 2023, **32**, 25–50.
- 24 X. Zhang, D. Zhang, X. Ni and H. Zheng, *Solid-State Electron.*, 2008, **52**, 245–248.
- 25 A. A. Raj and V. Biju, *Mater. Sci. Semicond. Process.*, 2017, **68**, 38–47.
- 26 P. R. Dubey, G. Kaur and R. Shukla, *Mol. Neurobiol.*, 2025, 1–20.
- 27 T. Ameh and C. Sayes, *Environ. Toxicol. Pharmacol.*, 2019, **71**, 103220.
- 28 M. Jiang, X. Tao, Y. Pang, Z. Qin, E. Song and Y. Song, *J. Hazard. Mater.*, 2024, **480**, 136416.
- 29 M. Q. Fang, *J. Chongqing Univ. Sci. Technol.*, 2006, **8**, 30–32.
- 30 J. Leitner, D. Sedmidubský, M. Lojka and O. Jankovský, *Materials*, 2020, **13**, 2878.
- 31 S. Nilsson, M. R. Nielsen, J. Fritzsche, C. Langhammer and S. Kadkhodazadeh, *Nanoscale*, 2022, **14**, 8332–8341.
- 32 S. Nilsson, D. Albinsson, T. J. Antosiewicz, J. Fritzsche and C. Langhammer, *Nanoscale*, 2019, **11**, 20725–20733.
- 33 Y. Zuo, A. Robador, M. Wickham and S. H. Mannan, *Corros. Sci.*, 2022, **209**, 110713.
- 34 S. R. Esa, R. Yahya, A. Hassan and G. Omar, *Ionics*, 2017, **23**, 319–329.
- 35 M. Watanabe, Y. Higashi and T. Tanaka, *Corros. Sci.*, 2003, **45**, 1439–1453.



36 G. Zhou, L. Luo, L. Li, J. Ciston, E. A. Stach and J. C. Yang, *Phys. Rev. Lett.*, 2012, **109**, 235502.

37 M. Li, M. T. Curnan, W. A. Saidi and J. C. Yang, *Nano Lett.*, 2022, **22**, 1075–1082.

38 X. Zhang, J. Han, J. J. Plombon, A. P. Sutton, D. J. Srolovitz and J. J. Boland, *Science*, 2017, **357**, 397–400.

39 S. J. Kim, Y. I. Kim, B. Lamichhane, Y.-H. Kim, Y. Lee, C. R. Cho, M. Cheon, J. C. Kim, H. Y. Jeong and T. Ha, *Nature*, 2022, **603**, 434–438.

40 D.-M. Ye, G.-Z. Li, G.-G. Wang, Z.-Q. Lin, H.-L. Zhou, M. Han, Y.-L. Liu and J.-C. Han, *Appl. Surf. Sci.*, 2019, **467**, 158–167.

41 K. Kim, K. N. Chaudhari, S. Kim, Y. Kim and K. S. Shin, *J. Ind. Eng. Chem.*, 2021, **95**, 388–396.

42 S. Zhou, X. Zeng, X. Yan, F. Xie, B. D. Fahlman, C. Wang and W. Li, *Appl. Surf. Sci.*, 2022, **604**, 154597.

43 M. M. Hasan, S. A. Tolba and N. K. Allam, *ACS Sustain. Chem. Eng.*, 2018, **6**, 16876–16885.

44 R. Navik, D. Xiao, Y. Gai, H. Tan and Y. Zhao, *Appl. Surf. Sci.*, 2020, **527**, 146694.

45 C.-A. Tseng, C.-C. Chen, R. K. Ulaganathan, C.-P. Lee, H.-C. Chiang, C.-F. Chang and Y.-T. Chen, *ACS Appl. Mater. Interfaces*, 2017, **9**, 25067–25072.

46 Y.-T. Lin, D.-W. Huang, P.-F. Huang, L.-C. Chang, Y.-T. Lai and N.-H. Tai, *Nanoscale Res. Lett.*, 2022, **17**, 79.

47 J. Wang, Z. Zhang, S. Wang, R. Zhang, Y. Guo, G. Cheng, Y. Gu, K. Liu and K. Chen, *Nano Energy*, 2020, **71**, 104638.

48 H. Ye, J. Chen, S. Wei, Y. Hu, Y. Wang, X.-Z. Fu and R. Sun, *J. Alloys Compd.*, 2023, **957**, 170398.

49 X. Shu, J. Feng, J. Liao, D. Zhang, R. Peng, Q. Shi and X. Xie, *J. Alloys Compd.*, 2020, **848**, 156556.

50 M. H. Kang, S. J. Lee, J. Y. Park and J. K. Park, *J. Alloys Compd.*, 2018, **735**, 2162–2166.

51 A. I. Quilez-Molina, S. Barroso-Solares, V. Hurtado-García, J. A. Heredia-Guerrero, M. L. Rodriguez-Mendez, M. Á. Rodríguez-Pérez and J. Pinto, *ACS Appl. Mater. Interfaces*, 2023, **15**, 20385–20397.

52 D. A. Marin-Silva, N. Romano, L. Damonte, L. Giannuzzi and A. Pinotti, *Int. J. Biol. Macromol.*, 2023, **242**, 124898.

53 J.-M. Chiu, I. Wahdini, Y.-N. Shen, C.-Y. Tseng, J. Sharma and Y. Tai, *ACS Appl. Energy Mater.*, 2023, **6**, 5058–5066.

54 I. Hong, Y. Roh, J. S. Koh, S. Na, T. Kim, E. Lee, H. An, J. Kwon, J. Yeo and S. Hong, *Adv. Mater. Technol.*, 2019, **4**, 1800422.

55 S. Lee, C. Wern and S. Yi, *Materials*, 2022, **15**, 1135.

56 S. Polat Genlik, D. Tigan, Y. Kocak, K. E. Ercan, M. O. Cicek, S. Tunca, S. Koylan, S. Coskun, E. Ozensoy and H. E. J. Unalan, *ACS Appl. Mater. Interfaces*, 2020, **12**, 45136–45144.

57 J. Kim, M. Kim, H. Jung, J. Park and Y. N. E. Lee, *Nano Energy*, 2023, **106**, 108067.

58 W. Li, L. Li, F. Li, K. Kawakami, Q. Sun, T. Nakayama, X. Liu, M. Kanehara, J. Zhang and T. Minari, *ACS Appl. Mater. Interfaces*, 2022, **14**, 8146–8156.

59 Y. Xu, B. Cui, X. Zhang, Y. Sun and B. Lin, *Surf. Interfaces*, 2024, **46**, 104137.

60 X. Li, J. Natsuki and T. Natsuki, *Mater. Charact.*, 2021, **172**, 110887.

61 G. Liu, J. Wang, Y. Ge, Y. Wang, S. Lu, Y. Zhao, Y. Tang, A. M. Soomro, Q. Hong and X. Yang, *ACS Nano*, 2020, **14**, 6761–6773.

62 H. Zhang, S. Wang, Y. Tian, Y. Liu, J. Wen, Y. Huang, C. Hang, Z. Zheng and C. Wang, *Chem. Eng. J.*, 2020, **390**, 124495.

63 K. Liu, Y. Li, H. Zhang and Y. Liu, *Appl. Surf. Sci.*, 2018, **439**, 226–231.

64 Z.-Q. Wang, C. Deng, B. Li, H.-Q. Luo, P. Hao, X. Liu, J.-G. Ma and P. Cheng, *Mater. Horiz.*, 2024, **11**, 1957–1963.

65 X. Tong, H. Hu, X. Zhao and Q. Tai, *Metallurgy Materials, Int. J. Miner. Metall. Mater.*, 2022, **29**, 557–562.

66 Y. Fang, B. Xu, S. Wang, H. Liu, J. Wang and M. Si, *Nanoscale*, 2024, **16**, 9748–9753.

67 S. Wu, M. Zou, X. Shi, Y. Yuan, W. Bai, M. Ding and A. Cao, *Adv. Mater. Technol.*, 2019, **4**, 1900470.

68 H.-f. Chen, J.-j. Wu, M.-y. Wu and H. Jia, *N. Carbon Mater.*, 2019, **34**, 382–389.

69 L. Zhao, J. Li, Z. Song, X. Wang and S. Yu, *ACS Appl. Nano Mater.*, 2023, **6**, 10658–10667.

70 R. Navik, X. Ding, T. Huijun, Y. Gai and Y. Zhao, *Appl. Mater. Today*, 2020, **19**, 100619.

71 Z. Hongfeng, A. El-Kott, A. E. Ahmed and A. Khames, *Arab. J. Chem.*, 2021, **14**, 103259.

72 Z. Yin, S. Chen, Y. Guan, Q. Ran, Q. Zhang, X. Yan, R. Jin, H. Yu, L. Li and J. Yu, *ACS Appl. Mater. Interfaces*, 2019, **11**, 5264–5275.

73 R. J. Pinto, J. M. Lucas, F. M. Silva, A. V. Girão, F. J. Oliveira, P. A. Marques and C. S. Freire, *J. Clean. Prod.*, 2019, **221**, 122–131.

74 L. Tian, L. Sun, B. Gao, F. Li, C. Li, R. Wang, Y. Liu, X. Li, L. Niu and Z. Zhang, *Nanoscale*, 2024, **16**, 1320–1330.

75 S.-Y. Xia, X.-J. Li, Y.-J. Guo, J.-J. Yuan, Z.-F. Sun, H.-J. Cao, S.-Y. Zhang, W.-Z. Cai, J.-T. Li and Z.-H. J. Zhang, *Rare Met.*, 2025, 1–18.

76 S.-Y. Xia, X.-J. Li, Y.-J. Guo, J.-J. Yuan, Z.-F. Sun, H.-J. Cao, S.-Y. Zhang, W.-Z. Cai, J.-T. Li and Z.-H. Zhang, *Rare Met.*, 2025, 1–18.

77 L. Lu, C. Zhu, F. Li, P. Wang, X. Kang, Y. Pei and M. Zhu, *Chin. J. Struct. Chem.*, 2024, **43**, 100411.

78 S. Yokoyama, I. Suzuki, K. Motomiya, H. Takahashi and K. Tohji, *Colloids Surf. A*, 2018, **545**, 93–100.

79 N. Sarwar, S. H. Choi, G. Dastgeer, U. B. Humayoun, M. Kumar, A. Nawaz, D. I. Jeong, S. F. A. Zaidi and D. H. Yoon, *Appl. Surf. Sci.*, 2021, **542**, 148609.

80 Y. M. Wang, X. C. Lin, K. M. Mo, M. Xie, Y. L. Huang, G. H. Ning and D. Li, *Angew. Chem., Int. Ed.*, 2023, **62**, e202218369.

81 A. Oliva-Puigdomenech, J. De Roo, J. Kuhs, C. Detavernier, J. C. Martins and Z. Hens, *Chem. Mater.*, 2019, **31**, 2058–2067.

82 M. I. Din, F. Arshad, Z. Hussain and M. Mukhtar, *Nanoscale Res. Lett.*, 2017, **12**, 1–15.

83 P. Sharma, M. Ganguly and A. Doi, *Nanoscale Adv.*, 2024, **6**(14), 3476–3493.

84 P. Zhang, Q. Sun, S. Fang, H. Guo, K. Liu, L. Zhang, Q. Zhu and M. Wang, *ACS Appl. Mater. Interfaces*, 2024, **17**, 1847–1860.



85 Y. Zhang, P. Zhu, G. Li, T. Zhao, X. Fu, R. Sun, F. Zhou and C.-P. Wong, *ACS Appl. Mater. Interfaces*, 2014, **6**, 560–567.

86 S. Hong, C. Liu, S. Hao, W. Fu, J. Peng, B. Wu and N. Zheng, *Flexible Electron.*, 2022, **6**, 17.

87 T. Zhang, F. Daneshvar, S. Wang and H.-J. Sue, *Mater. Des.*, 2019, **162**, 154–161.

88 Q. Xiang, R. Navik, H. Tan and Y. Zhao, *J. Alloys Compd.*, 2022, **914**, 165265.

89 H. Li, M. He, S. Meng, P. Wang, C. Yang, J. Yao, Z. Hu and Z. Li, *Inorg. Chem. Front.*, 2025, **16**, 960.

90 Z. Chen and K. A. Fichthorn, *Nanoscale*, 2021, **13**, 13529–13537.

91 D. Kumar, N. Jain, V. Jain and B. Rai, *Appl. Surf. Sci.*, 2020, **514**, 145905.

92 M. M. Kadhim, K. O. Alaboodi, S. K. Hachim, S. A. Abdulla, T. Z. Taban and A. M. J. Rheima, *J. Mol. Model.*, 2023, **29**, 27.

93 Y. Zhang, S. Zhang, B. Tan, L. Guo and H. Li, *J. Colloid Interface Sci.*, 2021, **604**, 1–14.

94 S. S. Han, A. Thacharon, J. Kim, K. Chung, X. Liu, W. S. Jang, A. Jetbyayeva, S. Hong, K. H. Lee and Y. M. Kim, *Adv. Sci.*, 2023, **10**, 2204248.

95 J. Graves, E. Latvytė, A. Greenwood and N. Emekwuru, *Ultrason. Sonochem.*, 2019, **55**, 25–31.

96 J. Qi, J. Zheng, T. Butburee, Q. Huang, H. Fang, Y. Wang, L. Zhou, D. Zhang, L. Zhang and S. Song, *Appl. Surf. Sci.*, 2024, **669**, 160451.

97 V. Cremers, G. Rampelberg, A. Barhoum, P. Walters, N. Claes, T. M. de Oliveira, G. Van Assche, S. Bals, J. Dendooven and C. J. S. Detavernier, *Surf. Coating. Technol.*, 2018, **349**, 1032–1041.

